ELSEVIER

Surface Science 307–309 (1994) 1148–1160

surface science

Invited paper

Adsorption on oxide surfaces: structure and dynamics

F. Winkelmann, S. Wohlrab, J. Libuda, M. Bäumer, D. Cappus, M. Menges, K. Al-Shamery, H. Kuhlenbeck, H.-J. Freund *

Lehrstuhl für Physikalische Chemie I, Ruhr-Universität Bochum, Universitätsstrasse 150, 44780 Bochum, Germany

(Received 20 August 1993)

Abstract

In contrast to metal surfaces, oxide surfaces have only been studied rather recently with surface science methods. We report on the preparation and electron spectroscopic investigations of thin, well ordered surfaces of clean, adsorbate covered and modified oxide films. We identify surface excited states of a NiO(100) surface via electron energy loss spectroscopy in the regime of electronic excitations. Adsorption on well ordered terraces and on defects can be distinguished by choosing proper probe molecules. As a model system to study the structure and reactivity of an oxide supported ultrathin metal film we have deposited Pt onto a thin Al_2O_3(111) film grown on a NiAl(110) substrate. CO adsorption and low temperature dissociation in contrast to the bulk Pt has been observed.

1. Introduction

Surface science has been and still is rather important to try to unravel the elementary steps of adsorption and reaction on single crystal surfaces at the atomic level. For certain reactions in heterogeneous catalysis the transfer of information from single crystal surfaces to explain the observed kinetics and reaction yields has been possible [1]. One of the most spectacular successes in this respect has been achieved for the ammonia synthesis from elemental nitrogen and hydrogen, i.e. the Haber–Bosch process [2]. The action of inhibitors and promotors on this surface reaction has been studied and some of the key factors influencing the reaction have been unraveled [3]. Even though oxide surfaces are equally or even more important in heterogeneous catalysis their surfaces have been studied to a much lesser extent with respect to adsorption [4]. There are several reasons for this situation, some of which are technical in nature and some are connected with the structure of oxides where defects play a much more important role as compared with metal surfaces [5]. For example, technical problems occur due to charging of the samples in electron spectroscopic experiments. Also, insulating samples are often hard to cool efficiently to liquid nitrogen and liquid helium temperatures. It has therefore been our goal to circumvent these problems by preparing thin, well ordered oxide films on metal substrates which do not charge upon electron impact or electron emissions and which may easily be cooled to low temperatures [6].

The structural problems on the other hand are intimately related to the stability and ill defined

* Corresponding author. Fax: +49 (234) 7094182.

SSDI 0039-6028(93)E0976-2

stoichiometry of some oxide surfaces. Fig. 1 indicates the situation for the oxide materials considered in this study by plotting the negative logarithm of the partial O_2 pressure at $T = 1000$ K required for equilibrium between different phases [7]. Effectively, this is the oxygen affinity of the 3d transition metals and their oxides. For example, Cr with an oxygen affinity of about 30 drops to a value below 0 as soon as the stoichiometry of Cr_2O_3, i.e. a metal-to-oxygen ratio of 1.5, is reached. The one-phase region is sharp for Ni, Co and Cr, while it is wide in the case of Fe in connection with FeO formation indicating the problem in stoichiometry to be expected with FeO films.

There is another factor that has to be taken into account if we discuss the stability of thin oxide layers, namely the crystallographic orientation of the film. Since many oxides are highly ionic compounds, the electrostatic part of the lattice energy becomes important when we consider different surface orientations. Fig. 2 schematically shows the arrangement of planes for a simple AB-type ionic solid and an A_2B-type ionic solid. The picture has been taken from Tasker's work [8]. The surfaces may be divided

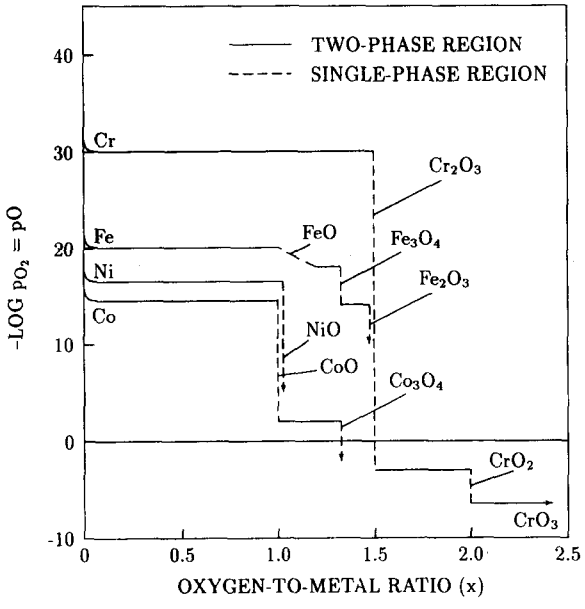

Fig. 1. Oxygen affinities for Fe, Co, Ni and Cr metal and oxides.

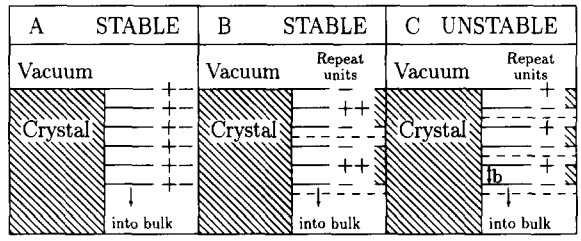

Fig. 2. Schematic representation of stable and unstable surfaces of AB-type and A_2B-type ionic crystals.

into non-polar and polar ones. A (100) surface of an AB-type solid is the typical case for a non-polar surface with vanishing dipole moments between the planes and full charge compensation within the planes. This arrangement leads to a converged, finite electrostatic surface energy. Upon going to the (111) surface of an AB-type lattice we create a polar surface. In this case there is no charge compensation within each layer and there is also a dipole moment within the repeat unit perpendicular to the surface. Consequently, the surface energy does not converge but increases unbound as the number of repeat units increases. Polar surfaces are, however, not necessarily unstable as illustrated for the A_2B-type solids. Even though there is no charge compensation in the plane, the dipole moment in the repeat unit perpendicular to the surface vanishes thus leading to a stable situation. Let us return to the polar surface of the AB-type system and consider the surface potential energy (V) in more detail.

$$V = 2\pi/S[Nb(2\sigma - 1) + (1 - \sigma)b], \qquad (1)$$

where S is the area of the unit cell. Eq. (1) gives this quantity as a function of the number of layers N, its separation b and the parameter σ which describes the difference in charge of the surface layer with respect to the bulk layer. It is quite obvious that the reduction of the surface charge such that $\sigma = 1/2$ leads to the disappearance of the first term in Eq. (1) and thus to a surface potential independent of the number of layers involved. While this is only a qualitative argument, it shows possible routes for the system to respond in order to stabilize polar AB-type surfaces. Surface charge reduction may be accomplished, for example by reconstructing, i.e. remov-

ing half of the ions, or by creation of steps. The latter leads to the coexistence of A-terminated and B-terminated patches on the same surface and thus to a microscopic charge compensation. Also, relaxations in the layer distances are expected to occur in the near surface region which could help to reduce the surface potential. In certain cases we may consider other routes of stabilization, e.g. on an oxygen-terminated surface. Upon adsorption of H^+, OH may form on the surface thus effectively reducing the surface charge.

While it is very hard to prepare polar surfaces on bulk single crystals, due to the above reasons, it turns out to be possible to do so in the case of thin films. Therefore, with the study of such thin films one has the possibility to complement investigations on non-polar surfaces prepared either via cleavage of bulk single crystals or also as thin films. Due to the relatively high energy of the polar surfaces, we expect a considerably higher chemical reactivity of such surfaces as compared with non-polar surfaces. This in turn may lead to interesting consequences for the discussion of heterogeneous reaction mechanisms.

There are other issues that are important to consider if we work with thin films:

(a) By choosing the appropriate substrates for growths and the ratios for metal and oxygen one may change the stoichiometry of the thin film and thus control to a certain extent the defect density and defect type of the film, which will influence, as we show below, the adsorption behaviour of the system.

(b) By varying the thickness of the film, it should be possible to study the influence of the metal substrate on the adsorption properties of the oxide surface. This may become particularly important if we deposit metal films or metal particles onto the thin oxide film, for example, in order to model dispersed metal catalysts on oxide supports.

2. Experimental

For this study three different UHV systems have been used. Two systems contain hemispherical electron energy analyzers rotable in two orthogonal planes for angle-resolved electron detection or fixed analyzers for X-ray photoelectron spectroscopy (XPS). One of these systems is additionally equipped with a hemispherical electron monochromator for angle-resolved EELS (electron energy loss spectroscopy). The third system contains an EELS setup consisting of a double pass cylindrical electron analyzer and monochromator. Additionally, all systems are equipped with LEED (low energy electron diffraction) systems, quadrupole mass spectrometers for residual gas analysis and TDS (thermal desorption spectroscopy), and ion guns for sample preparation.

The metallic samples, which were used for the preparation of the thin film oxides, were spot welded to two tungsten rods, which were connected to a liquid nitrogen reservoir. With this arrangement temperatures below $T = 100$ K could be reached. A tungsten filament was mounted behind the samples, which could be used for sample heating by electron impact or radiative heating. The samples were cleaned by repeated cycles of etching with Ne ions and annealing.

Studies on the oxidation of Ni have been performed rather early by Conrad et al. [9]. The NiO(100) and NiO(111) films have been prepared by oxidation of Ni(100) and Ni(111) single crystal surfaces in an oxygen atmosphere. NiO(100) was grown by cycles of oxidation with 1000 L (1 L = 10^{-6} Torr · s) of O_2 at elevated temperature (T = 570 K) followed by annealing at $T = 650$ K. These cycles were repeated until the LEED pattern indicated the formation of an ordered oxide film. The NiO(111) layers were prepared in a similar way. Both types of oxide films exhibit an appreciable amount of defects as indicated by the rather high background intensity and by the large half widths of the spots in the LEED patterns.

Immediately after preparation, the NiO(100) and NiO(111) films were found to be covered with OH groups, compatible with the H_2O and H_2 background pressure. These could be removed by annealing at $T \geqslant 600$ K. After cooling down, the formation of OH species could be observed again, indicating that the hydroxyl species were formed by a reaction of the oxide surfaces with the residual gas atmosphere. For

the isotope exchange experiments the hydroxylated oxide films were briefly flashed to $T = 600$ K in an atmosphere of 10^{-6} mbar of D_2O.

Some experiments have also been performed with a NiO(100) single crystal surface. The single crystal rod was cleaved in vacuo. This procedure resulted in a well ordered (100) surface with a very small concentration of defects which gave rise to a sharp (1×1) LEED pattern with low background intensity. On the cleaved surface no OH formation in detectable amounts was observed. Since the thermal contact of the single crystal rod to the sample holder was not as good as for the spot-welded metal samples, we used a helium cryostate for cooling purposes.

The aluminium oxide samples were prepared in the following way: after cleaning the NiAl(110) sample using sputtering and annealing cycles, the oxide film was prepared by admitting 1200 L of oxygen at $T = 550$ K into the chamber, and subsequent annealing to 1200 K as described in more detail elsewhere [10]. The quality of the resulting oxide film was documented by a set of sharp LEED spots with low background intensity.

Platinum has been deposited from a Pt filament. The coverage was controlled via a quartz balance and checked with XPS.

3. Results and discussion

Surfaces of transition metals and semiconductors are often characterized by typical surface states localized in the topmost layers of the systems. They may be identified via angle-resolved photoelectron spectroscopy through the observation of typical features in the valence electron region [11] and often through the so-called sur-

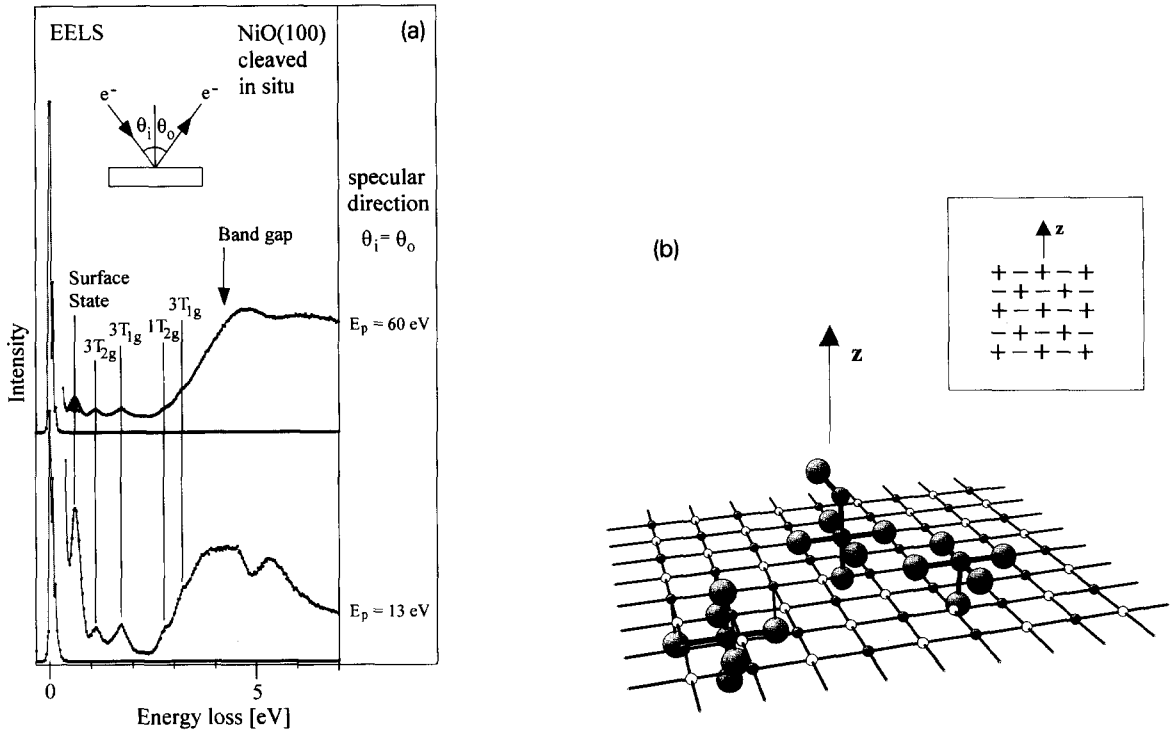

Fig. 3. (a) Electron energy loss spectra of an in situ cleaved NiO(111) surface at two different primary electron energies (E_p). (b) Schematic representation of a NiO single crystal lattice. A bulk NiO_6 coordination is compared with the clean surface site being occupied with an adsorbed NO molecule.

face chemical shift of the core ionizations of the atoms in the surface layer with respect to the bulk [12].

Similar information for transition metal oxides is not widely known, although there have been some reports on surface defect induced states in the literature [6,13].

We have found that electron energy loss spectroscopy in the range of the band gap of the oxide, i.e. up to about 4 eV excitation energy, is particularly well suited for the identification of such surface effects [10,14–20]. Fig. 3a shows the EEL spectrum of a vacuum-cleaved NiO(100) surface at two different primary electron energies [21]. The features marked with lines can be identified with known bulk transitions within the NiO band gap which is of charge transfer character and situated at 4.3 eV [22]. One particular feature is additionally observed at 0.6 eV excitation energy. Freitag et al. [15] have shown via ab initio calculations that this excitation is localized in the surface of the NiO(100) plane. Briefly, the situation is sketched in Fig. 3b: Each Ni^{2+} ion in the bulk is octahedrally coordinated by six oxygen O^{2-} ions. This ligand field leads to a splitting of the d-levels into a low lying t_{2g} and high lying e_g subsets. The t_{2g} subset is fully occupied, the e_g level is only half occupied forming a ^3A_g ground state. The lowest excitation leads to a configuration $t_{2g}^5 e_g^3$, which in turn results in several excited states, of which the $^3T_{2g}$ is the lowest lying at 1.1 eV excitation energy. At the surface, on the other hand, the Ni^{2+} ions are coordinated by only five O^{2-} ions in a ligand field of C_{4v} symmetry, thus effectively reducing the ligand field in particular perpendicular to the surface. Excitations involving transitions polarized perpendicularly to the surface are expected to occur at lower energies as compared with bulk transitions. The quantitative calculations show that the $^3A_{2g}$ ground state transforms according to $^3B_1$. The threefold degenerate $^3T_{2g}$ excited states splits into lower lying ^3E and a $^3B_2$ state which remains almost at the same energy as the $^3T_{2g}$ state in bulk NiO. Hence, the calculations assign the 0.6 eV feature to the ^3E state excited in the surface ligand field. Of course, other bulk transitions split into surface states. We refer to the original literature for details [14].

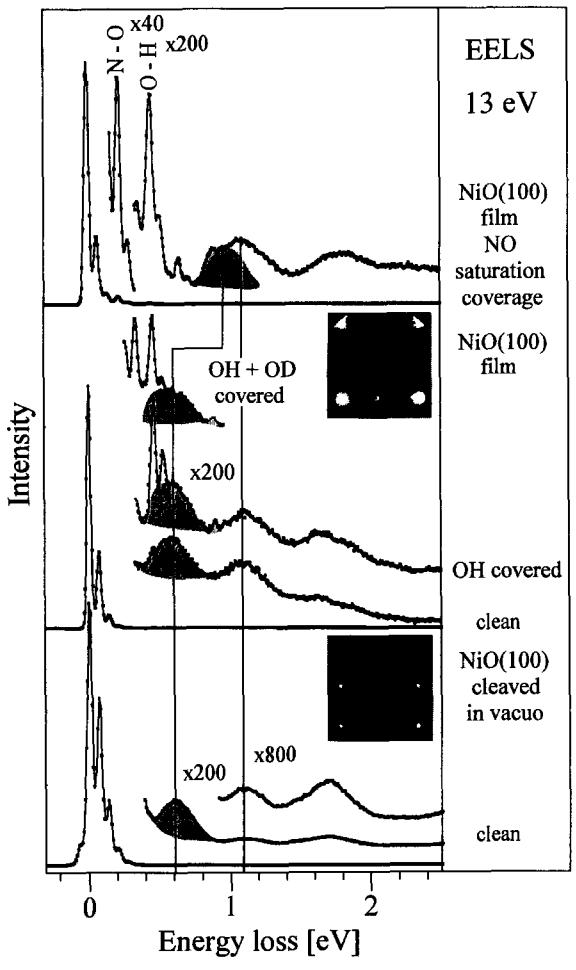

Fig. 4. Electron energy loss spectra of various NiO samples without and with adsorbates. The LEED patterns of the in situ cleaved single crystal and the grown film are shown as insets.

If we could coordinate a molecule from the gas phase to the surface Ni^{2+} ion, we would expect a shift of the transition to higher excitation energy because the ligand field is increased again. Fig. 4 shows what happens when we do the experiment. These experiments are performed on thin NiO(100) films because sample cooling is no problem. The lower two traces show the comparison of the relevant spectra in the appropriate energy range. Obviously, the two systems exhibit the same transitions, except for slight differences

in the relative intensities, which are connected with the fact that the film has a considerably higher defect density as compared with the bulk single crystal as revealed by the LEED spot sizes shown as insets. Such a NiO(100) film easily forms adsorbed OH groups as indicated by the sharp vibrational OH losses [14]. The assignment to OH losses is corroborated by the isotope exchange experiments as shown by the shifted OH losses in the third trace from the bottom. However, the surface excited state is not influenced in intensity by the presence of OH indicating that the hydroxyl groups are not located on the Ni terrace sites. We rather think that the OH groups are located at defect sites. This is supported by the fact that while OH groups adsorb easily on the NiO(100) film there is no trace of OH on the in situ cleaved single crystal even upon exposure to H_2O. NO, on the other hand, leads to a shift of the surface excited state towards higher energy as expected if another ligand is coordinated to the Ni^{2+} ions in the surface [15]. This is revealed by inspection of the topmost trace in Fig. 4. In this case the surface has been saturated by OH before NO was admitted. This finding corroborates the idea that OH and NO interact with different parts of the NiO(100) surface. From the experimental findings it is quite clear that NO coordinates to the Ni^{2+} terrace sites. We know in addition from NEXAFS measurements [23] that the NO molecular axis is tilted with respect to the surface normal by 45° (Fig. 3b). From TDS we know that the adsorption energy is about 0.5 eV [23].

While we have structural information on the NO surface site, we would also like to know more about the defect site of OH adsorption. In order to do so it is important to remember that we look at a NiO film with mainly (100) orientation. However, we know from SPA-LEED (spot-profile-analysis-LEED) and STM studies that about 25% of the film is defect covered [24,25]. Fig. 5a schematically shows how such a defect-containing NiO(100) film may look like [20]. (100) terraces are separated by (111) and (110) facets. The (111) terraces may be either Ni- or O-terminated. Via ab initio calculations on defect structures in the case of CO on MgO by Pacchioni and co-workers [26] one may find indications that edge atoms, where the metal atom is coordinated by O^{2-} ions similar to the situation on the (111) face, may bind molecules considerably stronger than terrace atoms. Therefore we studied a NiO(111) film, schematically shown in Fig. 5b. Here the main terraces are (111) oriented, either Ni- or O-terminated and the facets are either (110) or (100) oriented. We note in passing that the structural quality of the NiO(111) film is better than

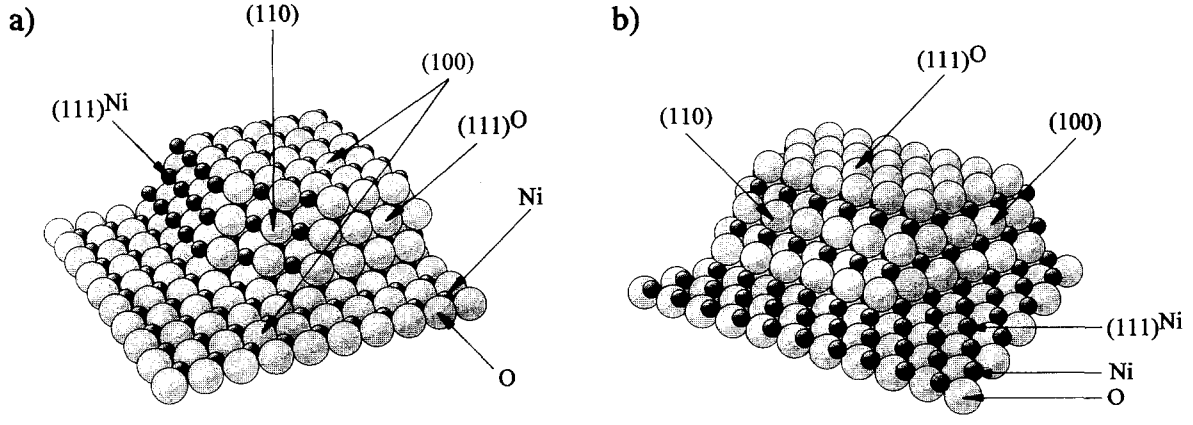

Fig. 5. (a) Schematic drawing of a facetted NiO(100) surface. The facets expose Ni-terminated, O-terminated (111) planes and (110) planes. (b) Schematic drawing of a facetted NiO(111) surface. The facets expose (100) and (110) planes. The lower and the upper (111) terraces are Ni- and O-terminated, respectively.

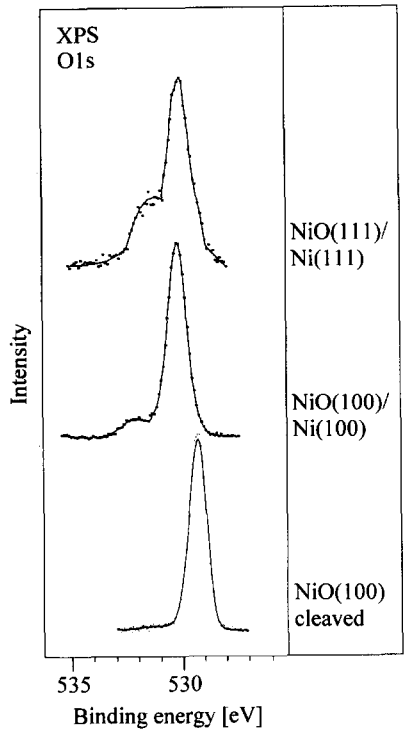

Fig. 6. X-ray photoelectron spectra of "clean" NiO samples in the range of the O 1s ionization. The spectra have been taken at grazing excidence.

the NiO(100) film [14]. Fig. 6 collects the O 1s spectra of the bulk NiO(100) cleavage plane in comparison with the O 1s spectra of the NiO(100) and NiO(111) films [20]. While the O 1s spectrum of the cleavage plane is a single symmetric line, the films show a shoulder at higher binding energy, which is due to the presence of OH at the surface. It is quite obvious in the spectra, taken at grazing electron exidence, that the OH concentration is considerably higher on the (111) surfaces as compared to the (100) surface. In fact, if we calculate the coverage quantitative, the OH coverage is by a factor of 3 larger on (111) as compared with (100). This shows that it is not unreasonable to assume the defects that adsorb OH are essentially NiO(111) facets. This is, of course, not a conclusive proof, but the results are, however, compatible with such an assignment. The presence of OH groups, in particular on the NiO(111) film, leads to a strong influence on the reactivity of the system towards other molecules [14]. Fig. 7 shows the comparison of the thermal desorption spectra of NO on NiO(100) and NiO(111) where the surfaces have been presaturated with OH (upper panel) and where the surface has been cleaned before NO adsorption. On the NiO(100) surface precovered with OH a single peak with a small shoulder is found [23]. Very similar results are observed for the OH-covered NiO(111) surface. While the dehydroxylated NiO(100) surface shows only a slightly changed desorption spectrum, the dehydroxylated NiO (111) surface exhibits a considerably different behaviour [13]. There are two equally intense desorption maxima at 195 and 280 K indicating different adsorption sites. At higher coverages we also observe a small desorption maximum at 465 K indicating decay of NO_2 or N_2O at the surface. This represents a simple example of how the

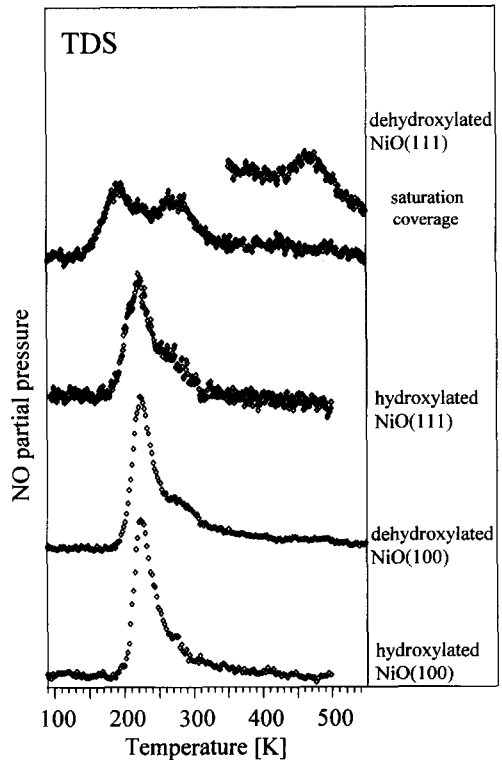

Fig. 7. Thermal desorption spectra of NO on NiO(100) and NiO(111) films ($\theta_{NO} = 0.1$ saturation coverage). The spectra were recorded for hydroxylated and for the dehydroxylated surfaces.

thermodynamically unstable surfaces may be stabilized by OH, effectively reducing the O^{2-} charge to OH^- and how the chemical reactivity of the surface is influenced. Such effects may be important in connection with catalytic reactions.

Another example of an oxide surface with completely different properties is represented by an Al_2O_3 film. This system is grown on a NiAl(110) single crystal surface as a thin (5 Å) very well ordered oxide film as judged by the SPA-LEED pattern with very sharp spots. This system has been chosen to represent a support material. Fig. 8 shows the global pattern and a close up indicating the double diffraction spots of the thin film [10]. Band structure measurements point to a hexagonally ordered first layer [10,18], and ISS shows that the surface is oxygen-terminated [27]. HREELS measurements indicate the presence of γ-Al_2O_3 with three phonon losses in contrast to α-Al_2O_3 with two phonon losses [18]. The HREEL spectrum of the clean surfaces is shown in Fig. 9 at the top. Such an Al_2O_3 surface may be used as a substrate to deposit metals onto it. We have deposited Pt onto the γ-Al_2O_3 surface and present in Fig. 9 the attenuation of the phonon losses with increasing Pt coverage [28]. The inset in Fig. 9 plots the phonon intensity decrease as a function of Pt coverage. It is clear that at less than a full monolayer coverage a metallic Pt overlayer has been formed on top of the Al_2O_3 film. LEED investigations show that at coverages above $\theta_{Pt} \approx 0.2$ the LEED pattern of the substrate is completely attenuated [29]. However, at lower coverages we can follow the structural changes occurring on the Al_2O_3 substrate. Fig. 10a shows a quasi-three-dimensional LEED pattern in the neighbourhood of the (0,0) reflex. It is obvious that upon Pt deposition (0.5 Å Pt) a shoulder forms which is isotropically distributed around the substrate spot. Note that the intensity of the oxide reflex from the clean substrate is strongly attenuated [29]. A one-dimensional cut through the pattern in Fig. 10a is

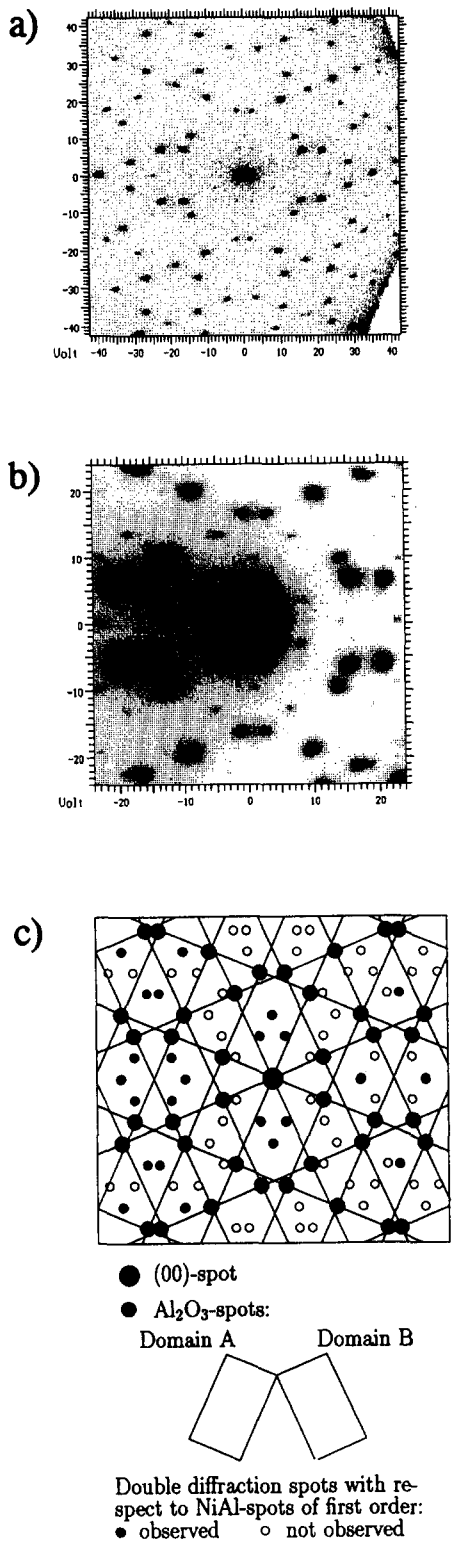

Fig. 8. SPA-LEED pattern of Al_2O_3(111)/NiAl(110). (a) Overview, (b) enlarged view with Al_2O_3 unit cell, (c) schematic representation indicating two domains.

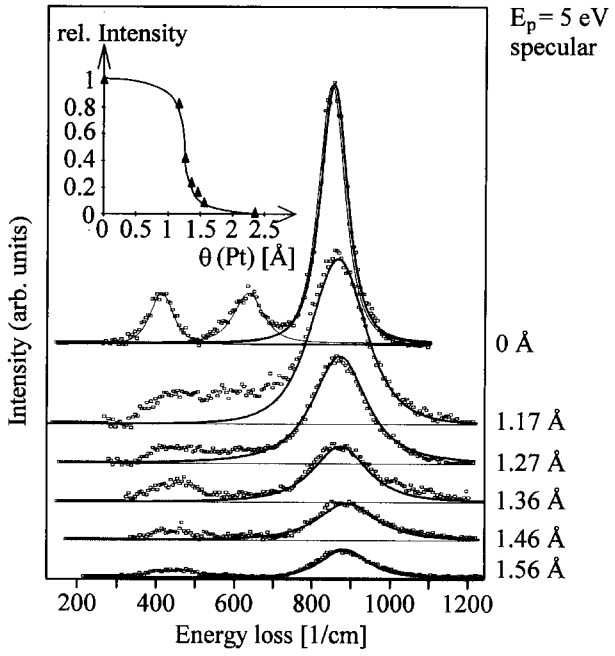

Fig. 9. Electron energy loss spectra of the phonon range of Al_2O_3(111)/NiAl(110). The spectrum of the clean system is compared with the spectra after depositing various amounts of Pt. The inset shows the intensity of the leading Al_2O_3 phonon as a function of metal layer thickness.

shown in Fig. 10b at the top. As discussed in detail elsewhere [29], it appears that through the action of the evaporated Pt the Al_2O_3 substrate is structurally modified. Two possibilities are compatible with the appearance of the shoulder as fitted to the experimentally observed line profile (Fig. 10b, lower trace): (i) each Pt atom modifies the Al_2O_3 structure within a rather well defined area or (ii) the Pt atoms only modify the substrate at particular structural positions, e.g. where Pt can migrate into the film. The analysis yields for a deposition of 0.25 Å Pt, an average size of the modified area of 10 Å diameter and an average distance of the modified areas of 10 Å establishing a coverage of the original oxide by modified areas of 0.5. The area of one modified region roughly corresponds to the area covered by an O^{2-} hexagon (seven ions) on the surface. Upon heat treatment of the layer the widths of shoulders decrease and the oxide reflexes lose more intensity (Fig. 10b, top). This indicates a further structural modification of the substrate. Parallel to the structural changes observed with LEED we have monitored the line shapes and intensities of the optical phonons of the substrate as shown in Fig. 9. The phonons of the system broaden and are stronlgy attenuated when we reach 1 Å Pt coverage [29].

The broadening and attenuation of the phonons (Fig. 9) is connected with the formation of a metallic Pt film on the dielectric substrate. Such a behaviour has also been observed before for other systems [30]. As may be deduced from the degree of attenuation of the Al_2O_3 phonons as shown in the inset in Fig. 9, a single monolayer of Pt leads to an almost complete quenching of the phonon losses indicating the formation of a 2 Å film with the response of a metal.

The adsorption properties of the thin Pt film are in certain aspects very similar to a Pt(111) surface as is revealed via HREELS and TDS. Fig. 11 shows the range of the CO stretching frequencies of the Pt/Al_2O_3 system dosed to saturation with CO. The observed frequency indicates CO molecules bound on-top on the surface [31]. At higher Pt coverages the band shifts and a second feature appears in the range of bridging CO sites. Due to the relatively low resolution we cannot decide at present how many different chemical species contribute to the broad feature present at the lowest Pt coverage. The existence of several species is very likely and also revealed through TDS measurements. A series is shown in Fig. 12. There is a broad structure between 350 and 550 K which shifts its maximum towards 450 K as the Pt coverage increases, and at high Pt coverage we find features known from TD spectra taken on Pt(111) [32] and stepped Pt(335) [33] surfaces shown for comparison. However, there is a pro-

Fig. 10. (a) Quasi-three-dimensional intensity distribution of the system Pt(0.5 Å)/Al_2O_3/ NiAl in the neighbourhood of the (0,0) reflex. (b) One-dimensional line profiles at two Pt coverages and two different substrate temperatures. A line fit is shown for the bottom profile.

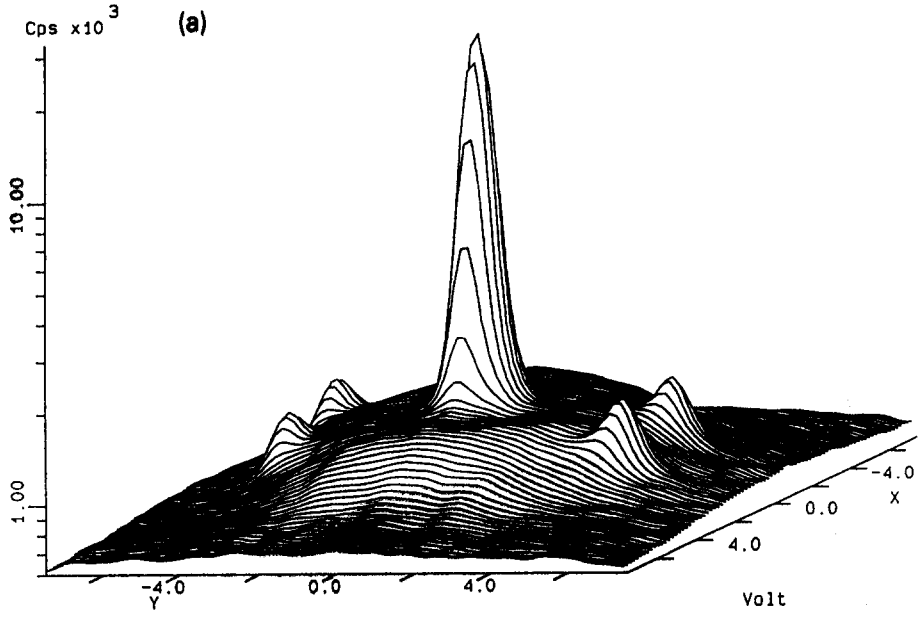
Cps x10 3
(a)
10.00
1.00
-4.0
0.0
4.0
Y
-4.0
0.0
4.0
X
Volt

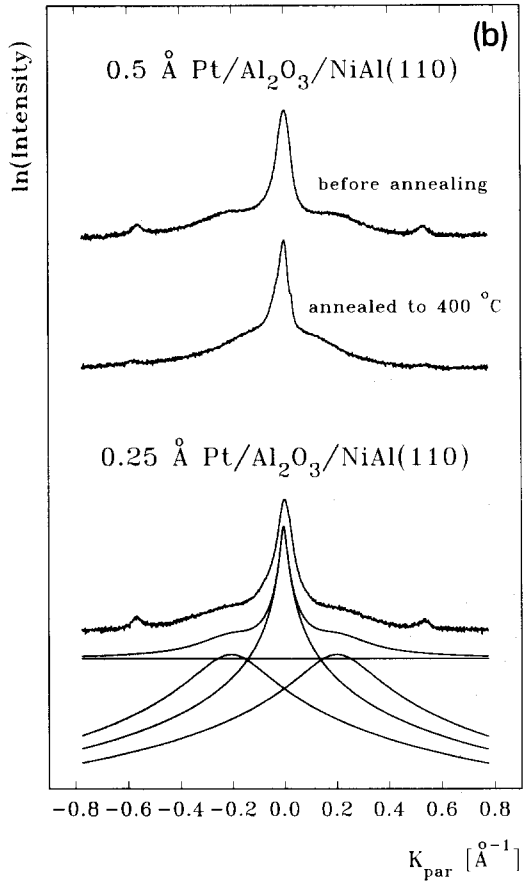
(b)
ln(Intensity)
0.5 Å Pt/Al2O3/NiAl(110)
before annealing
annealed to 400 °C
0.25 Å Pt/Al2O3/NiAl(110)
-0.8 -0.6 -0.4 -0.2 0.0 0.2 0.4 0.6 0.8
K par [Å-1]

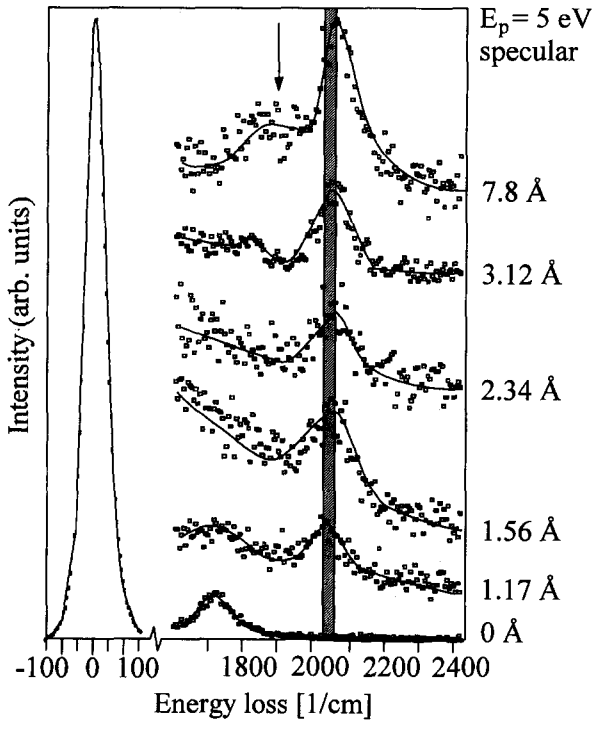

Fig. 11. Electron energy loss spectra in the range of the CO stretching frequencies for various Pt coverages and CO saturation coverage of the system Al_2O_3(111)/NiAl(110) (E_p = 5 eV).

nounced TDS feature slightly above a desorption temperature of 150 K which is not compatible with CO desorbing from metallic Pt. On the other hand we have found for CO desorbing from transition metal oxide surfaces maximum desorption temperatures between 100 and 200 K [14,16,23]. It is therefore not unlikely that these CO species desorb from sites where a Pt atom has been incorporated into the first layer of the Al_2O_3. By comparison with the clean NiAl(110) substrate and the completely Al_2O_3 covered NiAl(110) which are included in Fig. 12 it is clear that the desorption maximum around 150 K cannot be connected with the metallic NiAl(110) substrate. An investigation of the chemical shift of the Pt/Al_2O_3 system measured via XPS reveals that the Pt is oxidized when it diffuses into the substrate [22]. One may speculate that the defect structure of the γ-Al_2O_3 substrate helps to facilitate the diffusion of the relatively smaller Pt ions into the quasi-hexagonal top oxygen layer of the Al_2O_3.

We have just begun to study reactions with this Pt/Al_2O_3/NiAl system [28]. Fig. 13 shows C 1s photoelectron spectra taken with monochromatized Al Kα excitation of a Pt overlayer ($\theta_{Pt} \approx 0.7$ ML) at various substrate temperatures. At low temperatures (90 K) we find a signal typical for molecularly adsorbed CO. It is, in fact, very similar to the spectrum recorded for a thick Pt film,

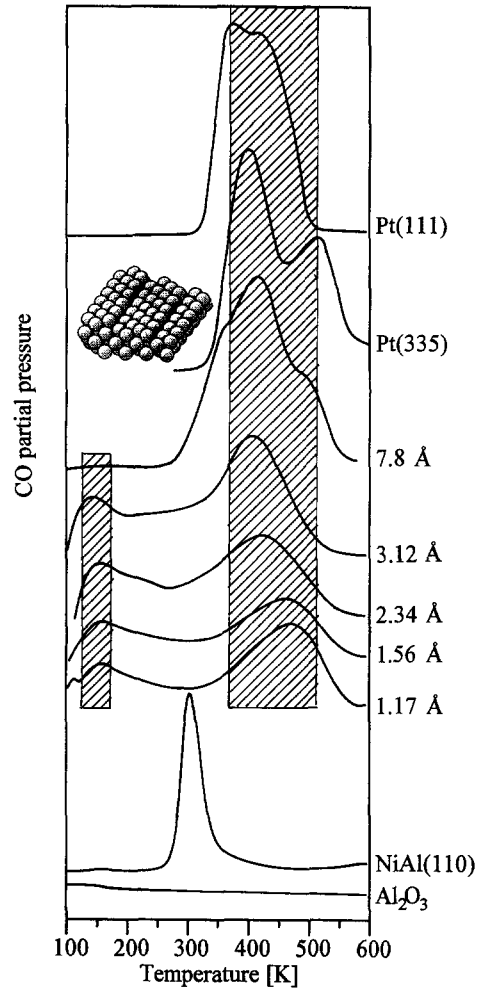

Fig. 12. Thermal desorption spectra of CO desorbing from Pt/Al_2O_3(111)/NiAl(110). For comparison the TD spectra taken from the literature [32,33] are included. The two spectra at the bottom refer to the clean NiAl(110) substrate and the clean Al_2O_3(111)/NiAl(110) system. The latter does not adsorb CO above 100 K.

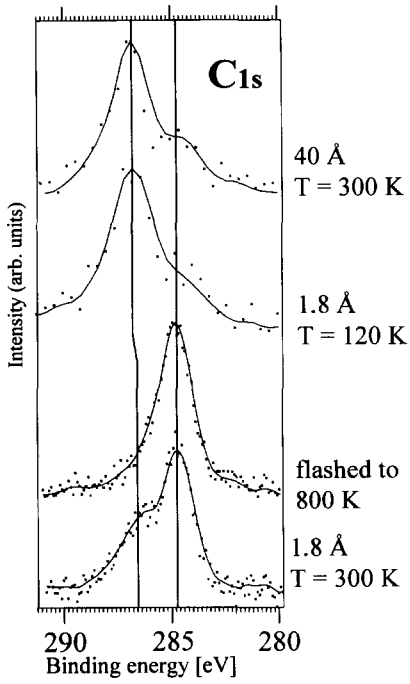

Fig. 13. C1s X-ray photoelectron spectra of the system $CO/Pt/Al_2O_3/NiAl(110)$ at various Pt coverages and substrate temperatures. CO saturation coverage has been reached.

shown for comparison. At 300 K, before desorption of CO from larger Pt aggregates occurs (see Fig. 12), we find a signal typical for adsorbed carbon at 284.8 eV in addition to the signal for molecularly adsorbed CO. The molecular species has desorbed above 600 K. The carbon signal remains even up to temperatures above 800 K. The cumulative information represents strong evidence that in contrast to CO on Pt single crystal surfaces [32,33] CO dissociates at rather low temperatures, in particular below room temperatures. This finding may have consequences for reaction of CO with coadsorbed species on such systems. It is our goal to study such systems in the near future.

4. Synopsis

Thin ordered oxide films may be used as model systems to study the geometric and electronic structure of ionic oxide materials. The greatest advantages of such thin film systems are represented by the possibilities to perform electron spectroscopic studies at low temperatures with even weakly adsorbed species present on the surface due to the avoided charging and heat conducting problems.

Also, thin films allow the preparation of ionic surfaces with different crystallographic orientations, in particular the polar surfaces, which are very difficult to prepare on bulk samples of ionic materials. It turns out that the presence of OH groups at these surfaces is important in stabilizing them. Removal of surface OH alters the reactivity of such surfaces considerably.

Thin oxide films of Al_2O_3 on NiAl(100) are well ordered and can be used as support materials for deposition of catalytically active transition metals. The structure of such systems may be studied with LEED and STM and its reactivity may be compared with those of the bulk transition metals. We find, for example, low-temperature dissociation of CO on deposited Pt films. This should be contrasted with the exclusively molecular adsorption on Pt bulk single crystals.

5. Acknowledgements

Our research has been supported by various agencies which are gratefully acknowledged: Deutsche Forschungsgemeinschaft, Ministerium für Wissenschaft und Forschung des Landes Nordrhein-Westfalen, Bundesministerium für Forschung und Technologie, European Communities and Fonds der Chemischen Industrie.

6. References

[1] P. Stoltze and J.K. Norskov, Phys. Rev. Lett. 55 (1985) 2502.
[2] G. Ertl, Angew. Chem. 102 (1990) 1258.
[3] M.P. Kiskinova, Poisoning and Promotion in Catalysis Based on Surface Science Concepts and Experiments, in: Studies in Surface Science and Catalysis, Vol. 70 (Elsevier, Amsterdam, 1989).
[4] H.H. Kung, Transition Metal Oxides: Surface Chemistry

and Catalysis, in: Studies in Surface Science and Catalysis, Vol. 45 (Elsevier, Amsterdam, 1990).
[5] V.E. Henrich and P.A. Cox, The Surface Science of Metal Oxides (Cambridge Univ. Press, Cambridge, 1993).
[6] H.-J. Freund and E. Umbach, Eds., Adsorption on Ordered Surfaces of Ionic Solids and Thin Films, in: Springer Series in Surface Science, Vol. 33 (Springer, Heidelberg, 1993).
[7] T.B. Reed, Free Energy of Formation of Binary Compounds (MIT, Cambridge, 1971).
[8] P.W. Tasker, J. Phys. C 12 (1979) 4977.
[9] H. Conrad, G. Ertl, J. Küppers and E.E. Latta, Solid State Commun. 17 (1975) 497.
[10] R.M. Jaeger, J. Libuda, M. Bäumer, K. Homann, H. Kuhlenbeck and H.-J. Freund, J. Electron Spectrosc. Relat. Phenom. 64/65 (1993) 217.
[11] P. Hermansson, M. Miosga and H. Neddermeyer, Surf. Sci. 84 (1979) 263.
[12] J.F. van der Veen, F.J. Himpsel and D.E. Eastman, Phys. Rev. Lett. 44 (1980) 189.
[13] W. Göpel, Progr. Surf. Sci. 20 (1985) 9.
[14] D. Cappus, C. Xu, D. Ehrlich, B. Dillmann, C.A. Ventrice, Jr., K. Al-Shamery, H. Kuhlenbeck and H.-J. Freund, Chem. Phys. 177 (1993) 533.
[15] A. Freitag, V. Staemmler, D. Cappus, C.A. Ventrice, Jr., K. Al-Shamery, H. Kuhlenbeck and H.-J. Freund, Chem. Phys. Lett. 210 (1993) 10.
[16] H. Kuhlenbeck, C. Xu, B. Dillmann, M. Hassel, B. Adam, D. Ehrlich, S. Wohlrab, H.-J. Freund, U.A. Ditzinger, H. Neddermeyer, M. Neuber and M. Neumann, Ber. Bunsenges. Phys. Chem. 96 (1992) 15.
[17] C. Xu, M. Hassel, H. Kuhlenbeck and H.-J. Freund, Surf. Sci. 258 (1991) 23.
[18] R.M. Jaeger, H. Kuhlenbeck, H.-J. Freund, M. Wuttig, W. Hoffmann, R. Franchy and H. Ibach, Surf. Sci. 259 (1991) 235.
[19] R.M. Jaeger, H. Kuhlenbeck and H.-J. Freund, Chem. Phys. Lett. 203 (1993) 41.
[20] D. Cappus, M. Menges, C. Xu, D. Ehrlich, B. Dillmann, C.A. Ventrice, Jr., J. Libuda, M. Bäumer, S. Wohlrab, F. Winkelmann, H. Kuhlenbeck and H.-J. Freund, J. Electron Spectrosc. Relat. Phenom., in press.
[21] St. Uhlenbrock, M. Neumann, D. Cappus and H.-J. Freund, in preparation.
[22] R.J. Powell and W.E. Spicer, Phys. Rev. B 2 (1970) 2182.
[23] H. Kuhlenbeck, G. Odörfer, R.M. Jaeger, G. Illing, M. Menges, Th. Mull, H.-J. Freund, M. Pöhlchen, V. Staemmler, S. Witzel, C. Scharfschwerdt, K. Wennemann, T. Liedtke and M. Neumann, Phys. Rev. B 43 (1991) 1969.
[24] M. Bäumer, D. Cappus, G. Illing, H. Kuhlenbeck and H.-J. Freund, J. Vac. Sci. Technol. A 10 (1992) 2407.
[25] M. Bäumer, D. Cappus, H. Kuhlenbeck, H.-J. Freund, G. Wilhelmi, A. Brodde and H. Neddermeyer, Surf. Sci. 253 (1991) 116.
[26] G. Pacchioni, T. Minerva and P.S. Bagus, Surf. Sci., in press.
[27] Th. Bertrams and H. Neddermeyer, unpublished data.
[28] F. Winkelmann, S. Wohlrab and H.-J. Freund, unpublished.
[29] J. Libuda, M. Bäumer and H.-J. Freund, unpublished.
[30] C.A. Ventrice, Jr., D. Ehrlich, E.L. Garfunkel, B. Dillmann, D. Heskett and H.-J. Freund, Phys. Rev. B 46 (1992) 12892.
[31] H. Ibach and D.L. Mills, Electron Energy Loss Spectroscopy and Surface Vibrations (Academic Press, New York, 1982).
[32] H. Steininger, S. Lehwald and H. Ibach, Surf. Sci. 123 (1982) 264.
[33] J.S. Luo, R.G. Tobin, D.K. Lambert, G.B. Fisher and C.L. DiMaggio, Surf. Sci. 274 (1992) 53.